

Ranging with High Accuracy and without Ambiguities

Sebastian Theiler, Manuel Stein and Josef A. Nossek
 Institute for Circuit Theory and Signal Processing
 Technische Universität München, Germany
 Email: {sebastian.theiler, manuel.stein, josef.a.nossek}@tum.de

Abstract—In order to perform precise radio-based ranging, the carrier phase information of the ranging signal needs to be exploited. State-of-the-art is to measure the phase as an independent parameter. Since the mapping from the carrier-phase to the time-delay parameter is ambiguous, measurements of multiple transmitters over multiple time instances can be combined in order to resolve the carrier phase ambiguities jointly. Here we restrict the discussion to the problem of delay estimation with a single transmitter on a single carrier frequency. Taking into account the dependency between the delay parameter and the carrier phase in the receive model, we show that under an ideal receive situation the delay parameter can be estimated unambiguously at ultra-high precision. To this end, we present a two step algorithm which consists of a particle filter (PF), precisely aligning to the grid of possible solutions and a subsequent histogram-based ambiguity resolution step. Numerical simulations for a GPS scenario show that the presented approach significantly outperforms the classical DLL/PLL-based approach.

Index Terms—precise ranging, carrier phase positioning, ambiguity resolution, satellite-based navigation and positioning

I. INTRODUCTION

Ranging at high accuracy is a core problem in various technical applications. High precision ranging can for example increase the efficiency and productivity in agriculture by using robots for pruning, weeding and crop-spraying. In marine navigation, ranging with high accuracy can help to enter a small port with big ships. Also the landing phase of an airplane can be automated by reliable ranging techniques. Ranging with radio systems is usually performed by measuring the propagation delay of an electro-magnetic wave with known structure. If the radio signal is transmitted on a high carrier frequency, it is well understood that the carrier phase conveys significant information about the delay parameter. However, as the mapping between phase and delay parameter is ambiguous, it is believed, that the carrier phase can only be exploited by combining measurements attained with different signal sources. In the application of satellite-based synchronization and navigation (GPS, GLONASS, Galileo, etc.), high precision is therefore achieved by performing three independent steps, depicted in Fig. 1. An acquisition algorithm delivers some initial knowledge about the range $r^{(l)}$ between transmitter l and the receiver for all available transmitters $l = 1, \dots, L$. Here this initial knowledge is characterized by a Gaussian random variable with mean $\mu_{\text{init}}^{(l)}$ and variance σ_{init}^2 . For each transmitter an individual tracking module then measures and



Fig. 1: Positioning

tracks the baseband delay and the carrier phase of the radio signal as independent parameters. In practice, this is done with two control loops, the delay-locked loop (DLL) and the phase-locked loop (PLL) [1]. With the DLL only a coarse ranging solution can be obtained [2]. The carrier phase $\zeta^{(l)}$ can be measured with much higher precision. However, the carrier phase is periodic with 2π and the measurement $\hat{\zeta}^{(l)}$ is, thus, only given by some fraction of a cycle, i.e. the integer number $\Psi^{(l)}$ of whole cycles is not known at the receiver

$$\hat{\zeta}^{(l)} = \omega_c \tau^{(l)} + 2\pi \Psi^{(l)} + e_{\zeta}^{(l)}, \quad (1)$$

where $\omega_c = 2\pi f_c$ is the carrier frequency, $\tau^{(l)} = \frac{r^{(l)}}{c}$ is the propagation-delay, c velocity of light and $e_{\zeta}^{(l)}$ the measurement error. Resolving the integer $\Psi^{(l)}$ precisely with measurements from one transmitter is not possible. Measurements from multiple transmitters and multiple time instances must be combined in order to resolve the ambiguity problem and obtain a solution \mathbf{x} with high accuracy [3]–[8]. In this work, we propose an approach to exploit the carrier phase information directly, i.e. we show that the ambiguity problem can be resolved directly and independently for each signal source in the tracking module. To this end, we model the noise-free part of the receive signal as an exact function of the propagation delay. In particular, the dependency between the carrier phase and the delay parameter is taken into account in an explicit way. Additionally, a statistical model for the temporal evolution of the delay parameter is used to align a tracking algorithm to the grid of possible delay solutions. Over subsequent observation blocks then a long integration ambiguity histogram (LIAH) is constructed with the likelihood function evaluated on the ambiguity grid. This allows to resolve the ambiguity issue and to output an ultra precise unbiased measurement of the delay parameter. The potential of the presented algorithm is demonstrated within a Global Navigation Satellite System (GNSS) scenario where each millisecond it becomes possible to measure the range between a fast moving satellite and a GPS receiver with millimeter accuracy.

II. OBSERVATION MODEL

Consider a scenario with one radio transmitter and a receiver. The transmitter emits an electro-magnetic wave of known periodic structure

$$x'(t) = s'(t) \cos(\omega_c t), \quad (2)$$

where $s'(t) \in \mathbb{R}$ is a periodic baseband signal and ω_c is the carrier frequency. The power of the transmitted signal $x'(t)$ is assumed to be normalized

$$\int_{-\infty}^{\infty} |X'(\omega)|^2 d\omega = 1, \quad (3)$$

where $|X'(\omega)|^2$ is the Fourier transform of the autocorrelation function of $x'(t)$. The signal at the receive sensor

$$\begin{aligned} y'(t) &= \gamma'(t)x'(t - \tau(t)) + n'(t) \\ &= \gamma'(t)s'(t - \tau(t)) \cos(\omega_c(t - \tau(t))) + n'(t). \end{aligned} \quad (4)$$

is characterized by a time-dependent propagation delay $\tau(t) \in \mathbb{R}$ and an attenuation $\gamma'(t) \in \mathbb{R}$, while the additive random noise $n'(t)$ is assumed to have flat power spectral density (PSD) $\Phi'(\omega) = N_0$. The receive signal $y'(t)$ is demodulated

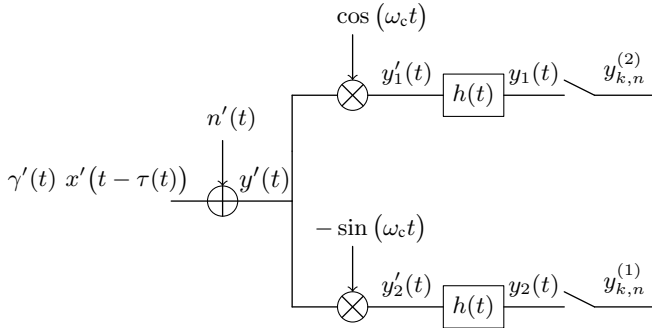


Fig. 2: RF Front-End

with two orthogonal functions

$$d_1(t) = \cos(\omega_c t) \quad (5)$$

$$d_2(t) = -\sin(\omega_c t) \quad (6)$$

oscillating at carrier frequency (see Fig. 2). The signals in the two demodulation channels can, hence, be written as

$$\begin{aligned} y'_1(t) &= y'(t)d_1(t) \\ &= \gamma(t)s'(t - \tau(t)) \left(\cos(\omega_c \tau(t)) \right. \\ &\quad \left. + \cos(2\omega_c t - \omega_c \tau(t)) \right) + n'_1(t) \end{aligned} \quad (7)$$

and

$$\begin{aligned} y'_2(t) &= y'(t)d_2(t) \\ &= \gamma(t)s'(t - \tau(t)) \left(-\sin(\omega_c \tau(t)) \right. \\ &\quad \left. - \sin(2\omega_c t - \omega_c \tau(t)) \right) + n'_2(t), \end{aligned} \quad (8)$$

where

$$n'_i(t) = d_i(t)n'(t), \quad i \in \{1, 2\}, \quad (9)$$

and

$$\gamma(t) = \frac{\gamma'(t)}{2}. \quad (10)$$

Note that $n'_1(t)$ and $n'_2(t)$ are uncorrelated, i.e. $E[n'_1(t)n'_2(t)] = 0, \forall t$. Moreover, the PSD of the additive white Gaussian noise components $n'_i(t)$ is given by $\Phi_i(\omega) = \frac{N_0}{2}, i \in \{1, 2\}$. The ideal low-pass filters $h(t)$ of the two channels are assumed to have one-sided bandwidth B . The filtered analog signals can, thus, be written as

$$\begin{aligned} y_1(t) &= y'_1(t) * h(t) \\ &= \gamma(t)s(t - \tau(t)) \cos(\omega_c \tau(t)) + n_1(t) \end{aligned} \quad (11)$$

$$\begin{aligned} y_2(t) &= y'_2(t) * h(t) \\ &= -\gamma(t)s(t - \tau(t)) \sin(\omega_c \tau(t)) + n_2(t), \end{aligned} \quad (12)$$

where

$$s(t) = s'(t) * h(t) \quad (13)$$

$$n_i(t) = n'_i(t) * h(t), \quad i \in \{1, 2\}, \quad (14)$$

with $*$ being the convolution operator. The signals of the two channels can be written in compact matrix-vector representation

$$\mathbf{y}(t) = \begin{bmatrix} y_1(t) \\ y_2(t) \end{bmatrix} = \gamma(t)\mathbf{b}(\tau(t))s(t; \tau(t)) + \mathbf{n}(t) \quad (15)$$

with

$$s(t; \tau(t)) = s(t - \tau(t)) \quad (16)$$

$$\mathbf{n}(t) = [n_1(t) \quad n_2(t)]^T \quad (17)$$

and

$$\mathbf{b}(\tau(t)) = [\cos(\omega_c \tau(t)) \quad -\sin(\omega_c \tau(t))]^T. \quad (18)$$

After filtering, the analog signals are sampled at a rate of $f_s = \frac{1}{T_s}$. In the following one observation block consists of N samples from each channel, i.e. $\mathbf{y}_k \in \mathbb{R}^{2N}$ is the observation in block k . The time-delay process is assumed to be approximately linear within one block

$$\tau(t) \approx \tau_k + \nu_k(t - t_k), \quad t \in [t_k; t_k + NT_s], \quad (19)$$

where τ_k is the time-delay of the first sample in block k and ν_k is the relative velocity (normalized by speed of light c) between receiver and transmitter in block k . The signal strength $\gamma(t)$ is assumed to be constant over one block

$$\gamma(t) = \gamma_k, \quad t \in [t_k; t_k + NT_s]. \quad (20)$$

For brevity of notation, the two parameter vectors

$$\boldsymbol{\theta}'_k = [\tau_k \quad \nu_k \quad \gamma_k]^T \quad (21)$$

$$\boldsymbol{\theta}_k = [\tau_k \quad \nu_k]^T \quad (22)$$

are introduced. The n -th sample in the k -th block is given by

$$\begin{aligned} \mathbf{y}_{k,n} &= \begin{bmatrix} y_{k,n}^{(1)} \\ y_{k,n}^{(2)} \end{bmatrix} = \begin{bmatrix} x_{k,n}^{(1)}(\boldsymbol{\theta}'_k) \\ x_{k,n}^{(2)}(\boldsymbol{\theta}'_k) \end{bmatrix} + \begin{bmatrix} n_{k,n}^{(1)} \\ n_{k,n}^{(2)} \end{bmatrix} \\ &= \mathbf{x}_{k,n}(\boldsymbol{\theta}'_k) + \mathbf{n}_{k,n} \\ &= \gamma_k \mathbf{b}_n(\boldsymbol{\theta}_k) s_{k,n}(\boldsymbol{\theta}_k) + \mathbf{n}_{k,n} \end{aligned} \quad (23)$$

with

$$s_{k,n}(\boldsymbol{\theta}_k) = s(t_k + (n-1)T_S - \tau_{k,n}(\boldsymbol{\theta}_k)) \quad (24)$$

$$\mathbf{n}_{k,n} = \begin{bmatrix} n_1(t_k + (n-1)T_S) \\ n_2(t_k + (n-1)T_S) \end{bmatrix} \quad (25)$$

and

$$\mathbf{b}_n(\boldsymbol{\theta}_k) = [\cos(\omega_c \tau_{k,n}(\boldsymbol{\theta}_k)) \quad -\sin(\omega_c \tau_{k,n}(\boldsymbol{\theta}_k))]^T, \quad (26)$$

where $\tau_{k,n}$ is the delay of the n -th sample in the k -th block

$$\tau_{k,n}(\boldsymbol{\theta}_k) = \tau_k + \nu_k(n-1)T_S. \quad (27)$$

The vector $\mathbf{b}_n(\boldsymbol{\theta}_k)$ can be decomposed

$$\mathbf{b}_n(\boldsymbol{\theta}_k) = \mathbf{T}(\tau_k) \mathbf{d}_n(\nu_k) \quad (28)$$

into a matrix

$$\mathbf{T}(\tau_k) = \begin{bmatrix} \cos(\omega_c \tau_k) & \sin(\omega_c \tau_k) \\ -\sin(\omega_c \tau_k) & \cos(\omega_c \tau_k) \end{bmatrix}, \quad (29)$$

which only depends on the delay parameter τ_k and a vector

$$\mathbf{d}_n(\nu_k) = \begin{bmatrix} \cos(\omega_c \nu_k(n-1)T_S) \\ -\sin(\omega_c \nu_k(n-1)T_S) \end{bmatrix}, \quad (30)$$

which only depends on the relative velocity ν_k . The receive signal can, thus, be modeled as

$$\mathbf{x}_{k,n}(\boldsymbol{\theta}'_k) = \gamma_k \mathbf{T}(\tau_k) \mathbf{d}_n(\nu_k) s_{k,n}(\boldsymbol{\theta}_k). \quad (31)$$

The vector of one observation block \mathbf{y}_k is defined as

$$\mathbf{y}_k = \begin{bmatrix} \mathbf{y}_{k,1} \\ \vdots \\ \mathbf{y}_{k,N} \end{bmatrix} = \begin{bmatrix} \mathbf{x}_{k,1}(\boldsymbol{\theta}'_k) \\ \vdots \\ \mathbf{x}_{k,N}(\boldsymbol{\theta}'_k) \end{bmatrix} + \begin{bmatrix} \mathbf{n}_{k,1} \\ \vdots \\ \mathbf{n}_{k,N} \end{bmatrix} = \mathbf{x}_k(\boldsymbol{\theta}'_k) + \mathbf{n}_k. \quad (32)$$

The noise \mathbf{n}_k is assumed to be uncorrelated. Hence, the noise covariance matrix is given as

$$\mathbf{R} = \mathbb{E}[\mathbf{n}_k \mathbf{n}_k^T] = BN_0 \mathbf{I}_{2N}, \quad (33)$$

where \mathbf{I}_{2N} is the identity matrix of dimension $2N$.

III. ML ESTIMATION WITH A SINGLE BLOCK

The receiver is interested in estimating the parameters of the receive signal in order to gain information about the propagation channel between transmitter and receiver. Using only one observation block for estimation, the maximum likelihood (ML) estimator is the best unbiased estimator [9]. The ML estimator is attained by solving the optimization

$$\hat{\boldsymbol{\theta}}'_k = \arg \max_{\boldsymbol{\theta}'_k \in \Theta'} f'_{\text{ML}}(\mathbf{y}_k; \boldsymbol{\theta}'_k), \quad (34)$$

where $f'_{\text{ML}}(\mathbf{y}_k; \boldsymbol{\theta}'_k) = p_{\mathbf{y}}(\mathbf{y}_k | \boldsymbol{\theta}'_k)$ and

$$p_{\mathbf{y}}(\mathbf{y}_k | \boldsymbol{\theta}'_k) = \frac{e^{\left(-\frac{1}{2BN_0}(\mathbf{y}_k - \mathbf{x}_k(\boldsymbol{\theta}'_k))^T(\mathbf{y}_k - \mathbf{x}_k(\boldsymbol{\theta}'_k))\right)}}{(2\pi BN_0)^N}. \quad (35)$$

The ML estimate for the signal strength γ_k can be computed in closed form as a function of $\boldsymbol{\theta}_k$ and \mathbf{y}_k and is given by

$$\hat{\gamma}_k(\boldsymbol{\theta}_k) = \frac{\sum_{n=1}^N \mathbf{y}_{k,n}^T \mathbf{T}(\tau_k) \mathbf{d}_n(\nu_k) s_{k,n}(\boldsymbol{\theta}_k)}{\sum_{n=1}^N (s_{k,n}(\boldsymbol{\theta}_k))^2}. \quad (36)$$

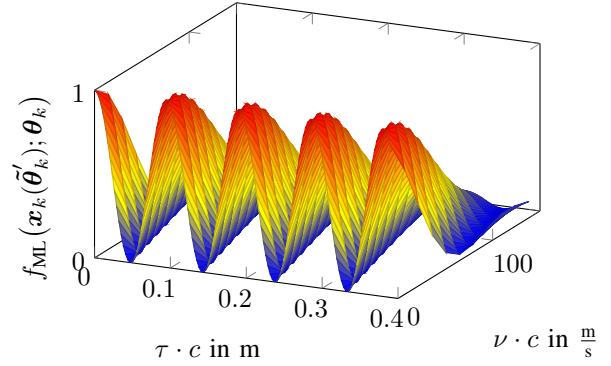


Fig. 3: ML Function

Substituting γ_k in the ML function results in a compact version

$$f_{\text{ML}}(\mathbf{y}_k; \boldsymbol{\theta}_k) = \frac{\left(\sum_{n=1}^N \mathbf{y}_{k,n}^T \mathbf{T}(\tau_k) \mathbf{d}_n(\nu_k) s_{k,n}(\boldsymbol{\theta}_k)\right)^2}{\sum_{n=1}^N (s_{k,n}(\boldsymbol{\theta}_k))^2} \quad (37)$$

and the problem can be reformulated

$$\hat{\boldsymbol{\theta}}_k = \arg \max_{\boldsymbol{\theta}_k \in \Theta} f_{\text{ML}}(\mathbf{y}_k; \boldsymbol{\theta}_k). \quad (38)$$

Note that only the maximization with respect to τ_k and ν_k is required, while the ML estimate for γ_k can be computed in closed form with the solution $\hat{\boldsymbol{\theta}}_k$. In Fig. 3, the normalized noise-free ML function $f_{\text{ML}}(\mathbf{x}_k(\tilde{\boldsymbol{\theta}}'_k); \boldsymbol{\theta}_k)$ with $\tilde{\boldsymbol{\theta}}'_k = [0 \ 0 \ 1]^T$ is plotted. A GPS-signal (C/A L1, Sat. 1)

$$s'(t) = \sum_{m=-\infty}^{\infty} [\mathbf{b}]_{\text{mod}(m,M)} g(t - mT_C) \quad (39)$$

with block length $N = 2046$ and chip duration $T_C = 977.53$ ns is used, where $\mathbf{b} \in \{-1, +1\}$ is a sequence of $M = 1023$ binary symbols, each of duration T_C , $\text{mod}(\cdot)$ is the modulo operator and $g(t)$ is a bandlimited transmit pulse. The carrier frequency is given as $f_c = 1575.42$ MHz. The one-sided bandwidth of the ideal low-pass filter at the receiver is equal to $B = T_C^{-1} = 1.023$ MHz. The sampling frequency is chosen according to the sampling theorem $f_s = 2B = 2.046$ MHz. The ML function is plotted in a range from 0 m to 0.4 m in τ_k -direction. There is no clear global maximum within this range, however, there are many local maxima. The distance between two neighboring maxima is half the wavelength $\Delta = \frac{c}{2f_c} = 0.0951$ m as the sign of the signal amplitude is not known at the receiver. As the height of the local maxima decays slowly in the direction of τ_k , the multi-modal shape of the ML function makes estimation with one observation block impossible. The idea of the following sections is to resolve this ambiguity issue with the help of a likelihood histogram which is constructed over a long integration time.

IV. NEARLY CONSTANT VELOCITY MODEL

In order to realize a long integration time within a dynamic scenario, the temporal evolution of the channel parameters has to be modeled precisely. Here an autoregressive model of first order is used

$$\boldsymbol{\theta}_{k+1} = \begin{bmatrix} \tau_{k+1} \\ \nu_{k+1} \end{bmatrix} = \mathbf{F} \boldsymbol{\theta}_k + \mathbf{w}_k, \quad (40)$$

where the matrix $\mathbf{F} \in \mathbb{R}^{2 \times 2}$ is the process matrix and \mathbf{w}_k is additive process noise with the covariance matrix

$$\mathbb{E}[\mathbf{w}_k \mathbf{w}_k^T] = \mathbf{Q} \in \mathbb{R}^{2 \times 2}. \quad (41)$$

This simple model turns out to be quiet accurate for practical GNSS scenarios. A meaningful assumption for practical scenarios is that the first derivative $\dot{\tau}(t)$ of the continuous time-delay process $\tau(t)$ given in (19) is nearly constant over the duration of one block. Consequently, higher order derivatives are almost equal to zero and the second order derivative $\ddot{\tau}(t)$ can be modeled as a zero mean white noise process $\ddot{\tau}(t) = w(t)$ with

$$\mathbb{E}[w(t)w(t')] = \sigma_w^2 \delta(t - t'). \quad (42)$$

The process matrix \mathbf{F} is then given as [10]

$$\mathbf{F} = \begin{bmatrix} 1 & T \\ 0 & 1 \end{bmatrix}, \quad (43)$$

where $T = t_{k+1} - t_k$ is the duration of one block, i.e. $T = NT_S$ and the covariance matrix \mathbf{Q} as

$$\mathbf{Q} = \sigma_w^2 \begin{bmatrix} \frac{T^3}{3} & \frac{T^2}{2} \\ \frac{T^2}{2} & T \end{bmatrix}. \quad (44)$$

V. PRECISE DELAY ESTIMATION WITH AMBIGUITY RESOLUTION

Apart from the observation model (32) and the process model (40), the prior knowledge from the acquisition algorithm is assumed to be Gaussian, i.e. $\tau_1 \sim \mathcal{N}(\mu_{\text{init},\tau}, \sigma_{\text{init},\tau}^2)$ and $\nu_1 \sim \mathcal{N}(\mu_{\text{init},\nu}, \sigma_{\text{init},\nu}^2)$. Combining all available information, it is possible to estimate and track the time-delay process $\tau(t)$ with very high accuracy. The proposed low-complexity estimation process consists of two steps for each block. The first step estimates and tracks one arbitrary time-delay ambiguity $\hat{\tau}_{\mathcal{A},k}$ with a particle filter (PF). Moreover, an estimate for the relative velocity $\hat{\nu}_k$ is provided. The second step exploits the structural information of the likelihood function by updating a likelihood histogram formed on a subset of points on the ambiguity grid \mathcal{A}_k . Based on this long integration ambiguity histogram (LIAH) the algorithm finally decides for the most probable time-delay solution $\hat{\tau}_k$.

A. Ambiguity Grid Alignment with a Particle Filter

The optimal estimator for the considered estimation problem is the conditional mean estimator (CME). Since our observation model shows severe non-linearities, the CME can not be stated in closed form. Hence, suboptimal approaches need to be used. An estimation method, which approximates the CME and is able to handle strong non-linearities, is particle filtering [10] [11]. Note that the PF is identical to the CME only for an infinite number of particles. However, a large number of particles results in high computational complexity. In order to guarantee a correct and precise delay-estimation with a small number of particles, step 1 only focuses on finding one arbitrary ambiguity. Therefore, the particles are initialized as

$$\tau_1^j \sim \mathcal{U}[\mu_{\text{init},\tau} - 0.5\Delta, \mu_{\text{init},\tau} + 0.5\Delta] \quad (45)$$

$$\nu_1^j \sim \mathcal{N}(\mu_{\text{init},\nu}, \sigma_{\text{init},\nu}^2) \quad (46)$$

for $j = 1, \dots, J$, where J is the number of used particles. Note that the time-delay particles are initialized uniformly in the range of one ambiguity. With this initialization, it is possible to estimate and track one ambiguity with high accuracy. The weight w_k^j of particle j is updated

$$w_k^j \propto w_{k-1}^j p_{\mathbf{y}}(\mathbf{y}_k | \boldsymbol{\theta}_k^j, \hat{\gamma}_k(\boldsymbol{\theta}_k^j)) \quad (47)$$

exploiting the observation \mathbf{y}_k of block k . Note that the weights are initialized uniformly, i.e. $w_0^j = \frac{1}{J}$ and are normalized in every step such that $\sum_{j=1}^J w_k^j = 1$. The tracking estimates are

$$\hat{\tau}_{\mathcal{A},k} = \sum_{j=1}^J w_k^j \tau_k^j \quad (48)$$

$$\hat{\nu}_k = \sum_{j=1}^J w_k^j \nu_k^j. \quad (49)$$

In every block the effective sample size

$$J_{\text{eff}} = \frac{1}{\sum_{j=1}^J w_k^j} \quad (50)$$

is computed [12]. If $J_{\text{eff}} < 0.5 \cdot J$, a resampling and roughening step is needed to guarantee the stability of the PF [14] [15]. Here systematic resampling [13] is used. The process model is used to update the particles

$$\boldsymbol{\theta}_{k+1}^j = \mathbf{F}\boldsymbol{\theta}_k^j + \mathbf{w}_k^j, \quad j \in \{1, \dots, J\}. \quad (51)$$

B. Ambiguity Resolution with LIAH

In the second step the structural information of the likelihood function is exploited. As the distance Δ between two neighboring ambiguities is known, the positions of all ambiguities, referred to as the ambiguity grid \mathcal{A}_k , can be estimated from $\hat{\tau}_{\mathcal{A},k}$. In the following the algorithm only considers the ambiguities within the interval

$$[\hat{\tau}_{\mathcal{A},k} - \epsilon\sigma_{\text{init},\tau}, \hat{\tau}_{\mathcal{A},k} + \epsilon\sigma_{\text{init},\tau}]. \quad (52)$$

Note that there is a trade-off between complexity and reliability which needs to be taken into account when choosing the design parameter ϵ . The probability that the true ambiguity, i.e. the time-delay τ_k , is within the interval

$$[\mu_{\text{init},\tau} - \epsilon\sigma_{\text{init},\tau}, \mu_{\text{init},\tau} + \epsilon\sigma_{\text{init},\tau}] \quad (53)$$

can be computed with the initial knowledge of the acquisition. The core part of the presented delay estimation process consists of different stages. In every stage the likelihood of a fixed number $A \geq 5$ of ambiguities out of the grid \mathcal{A}_k is tested. Without loss of generality, A is assumed to be odd. Within one stage the algorithm decides for one of the A ambiguities. The search is refined in the next stage. The A ambiguities for the first stage are

$$a_k^i = \text{round}\left(\left(-1 + (i-1)\frac{2}{A-1}\right)a_{\text{max}}\right) \quad (54)$$

with $\text{round}(\cdot)$ being the rounding operator, $i \in \{1, \dots, A\}$ and

$$a_{\text{max}} = \max\left(\left[\frac{\epsilon\sigma_{\text{init},\tau}}{\Delta}\right], \frac{A-1}{2}\right), \quad (55)$$

where $\lceil \cdot \rceil$ is the ceiling operator, i.e. the time-delay values

$$a_k^i \Delta + \hat{\tau}_{\mathcal{A},k}, \quad i \in \{1, \dots, A\} \quad (56)$$

are checked. In order to decide for one of these ambiguities, a probability measure p_k^i is introduced and assigned to each of the tested ambiguities. The likelihood histogram p_k^i is initialized $p_0^i = \frac{1}{A}$, $i \in \{1, \dots, A\}$ and updated in each block

$$p_k^i \propto p_{k-1}^i p_{\mathbf{y}_k}(\mathbf{y}_k | \hat{\boldsymbol{\theta}}_k^i, \hat{\gamma}_k(\hat{\boldsymbol{\theta}}_k^i)), \quad (57)$$

with

$$\hat{\boldsymbol{\theta}}_k^i = [a_k^i \Delta + \hat{\tau}_{\mathcal{A},k} \quad \hat{\nu}_k]^T, \quad (58)$$

where $\hat{\tau}_{\mathcal{A},k}$ and $\hat{\nu}_k$ are the estimates of the aligning filter. The histogram is then normalized such that $\sum_{i=1}^A p_k^i = 1$. The delay parameter can be determined with the histogram

$$\hat{\tau}_k = a_k^{i^*} \Delta + \hat{\tau}_{\mathcal{A},k}, \quad (59)$$

where $i^* = \arg \max_{i \in \{1, \dots, A\}} p_k^i$. Clearly, the true ambiguity needs not to be among the tested ambiguities in the first stage if the initial search interval is wider than A ambiguities. In order to find the true ambiguity, the search needs to be refined. Thus, a counter c_k^i , $i = 1, \dots, A$, is introduced and initialized with zero, $c_0^i = 0, \forall i$. Every time $p_k^i > \rho$, where $\frac{1}{A} < \rho < 1$, c_k^i is incremented by one. If a block is reached where c_k^i exceeds the design parameter $C \in \mathbb{R}$, the algorithm decides for ambiguity a_k^i and refines the search on the ambiguity grid. The particles τ_k^i of the grid aligning filter are shifted

$$\tau_k^j \leftarrow \tau_k^j + a_k^i \Delta, \quad (60)$$

i.e. also the estimate of the ambiguity $\tau_{\mathcal{A},k}$ is shifted

$$\hat{\tau}_{\mathcal{A},k} \leftarrow \hat{\tau}_{\mathcal{A},k} + a_k^i \Delta, \quad (61)$$

and a_{\max} is updated as

$$a_{\max} = \max \left(\chi, \frac{A-1}{2} \right) \quad (62)$$

with

$$\chi = \max_{u,v \in \{1, \dots, A\}} |a^u - a^v| \quad (63)$$

under the constraint $|u - v| = 1$. The interval which is considered in the following blocks is $[\hat{\tau}_{\mathcal{A},k} - a_{\max} \Delta, \hat{\tau}_{\mathcal{A},k} + a_{\max} \Delta]$. The tested ambiguities are computed as stated in (54). Note that if $a_{\max} = \frac{A-1}{2}$ no further refinement is necessary since all ambiguities in the considered interval are tested.

VI. SIMULATIONS

For the simulations a simple two-dimensional GNSS scenario depicted in Fig. 4 is considered. The receiver is positioned on a circle with radius R_E and center M. The receiver Rx is assumed to be static. The transmitter Tx moves on a circular orbit around the center M. If the transmitter is in the zenith, the distance between transmitter and receiver is h . The range $r(t)$ between transmitter and receiver for this scenario depends on the angle $\alpha(t) = \angle(\mathbf{R}_x, \mathbf{M}, \mathbf{T}_x)$ which is given as

$$\alpha(t) = \alpha_0 - 2\pi \frac{t}{T_0}, \quad (64)$$

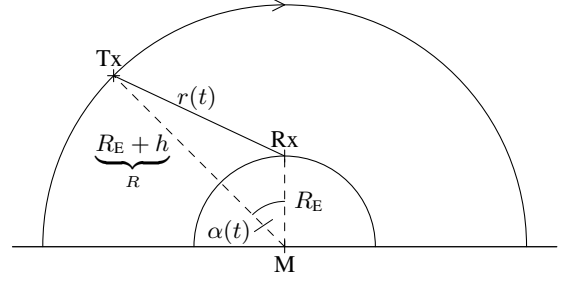


Fig. 4: Scenario

where T_0 is the circulation time of the transmitter Tx and $\alpha_0 = \alpha(0)$. Applying the law of cosine results in

$$r(t) = \sqrt{R_E^2 + R^2 - 2R_ER \cos(\alpha(t))} \quad (65)$$

for the range between transmitter and receiver, where $R = R_E + h$. The velocity is given by

$$\dot{r}(t) = \frac{R_ER \sin(\alpha(t)) \dot{\alpha}(t)}{r(t)} \quad (66)$$

with $\dot{\alpha}(t) = -\frac{2\pi}{T_0}$. For our simulations, the geometry is chosen according to a GPS scenario. $R_E = 6371 \cdot 10^3$ m is equal to the radius of the earth. $T_0 = 11$ h 58 min and $h = 20200 \cdot 10^3$ m are chosen according to the satellites of GPS, $\alpha_0 = \frac{\pi}{4}$. The parameter σ_w^2 of the nearly constant velocity model is determined with a least squares approach. For our scenario this results in $\sigma_w^2 = 2.6279 \cdot 10^{-14}$. The GPS-signal $s'(t)$ (39), the bandwidth B , the carrier frequency f_c and the sampling frequency are chosen as described in section III. The signal strength is assumed to be 55 dB-Hz. The initial uncertainty of the acquisition is

$$\sigma_{\text{init},\tau} = 75 \text{ m}, \quad (67)$$

$$\sigma_{\text{init},\nu} = 50 \frac{\text{m}}{\text{s}}. \quad (68)$$

The design parameters for the algorithm are $\epsilon = 3.5$, $A = 9$, $J = 100$, $\rho = 0.99$ and $C = 10$. In Fig. 5, the absolute value of the bias

$$\text{BIAS}_k = \mathbb{E}[\tau_k - \hat{\tau}_k], \quad (69)$$

the mean square error (MSE)

$$\text{MSE}_k = \mathbb{E}[(\tau_k - \hat{\tau}_k)^2] \quad (70)$$

and the variance

$$\text{VAR}_k = \text{MSE}_k - \text{BIAS}_k^2 \quad (71)$$

are measured for the estimation via LIAH with 250 realizations. It is observed, that the RMSE decreases to millimeter level within 1000 observation blocks ($\sqrt{\text{MSE}_{1000}} \approx 10^{-3}$ m). Apart from that, the estimation result is unbiased, i.e.

$$\text{BIAS}_k^2 \ll \text{MSE}_k \quad (72)$$

for k sufficiently large. As a reference, the range estimation result attained with a standard DLL/PLL approach, which is described and implemented in [16], is plotted in Fig. 6. The

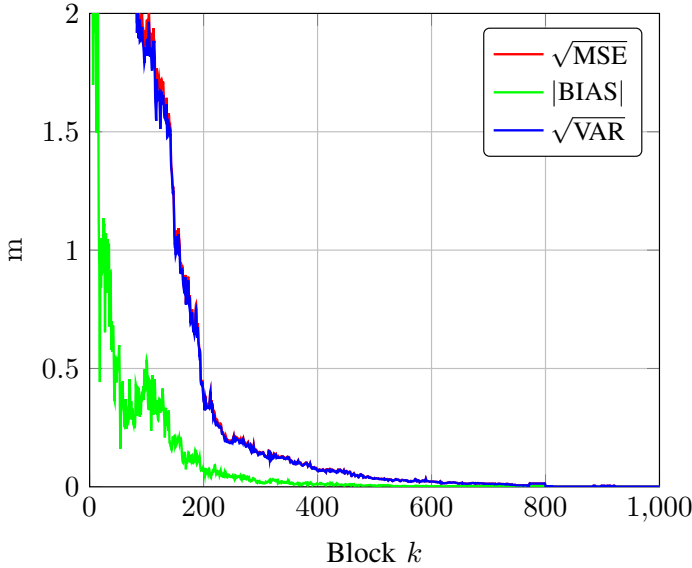


Fig. 5: Precise Histogram-based Approach

DLL/PLL damping ratio is 0.7 and the DLL bandwidth is 2 Hz, respectively. The PLL bandwidth is 25 Hz and the DLL correlator spacing is $0.5T_C$. 2500 realizations are used to measure the MSE, bias and variance. It can be observed that it is possible to estimate the range with the accuracy of a few meters with this standard approach. Interestingly, the mean square error (MSE)

$$\text{MSE}_k = \text{BIAS}_k^2 + \text{VAR}_k \quad (73)$$

of this state-of-the-art method is dominated by the bias, i.e. a systematic estimation error. Ignoring this error and considering the variance, it is possible to estimate the range on meter-level ($\sqrt{\text{VAR}_{1000}} \approx 2.0$ m) with this classical approach.

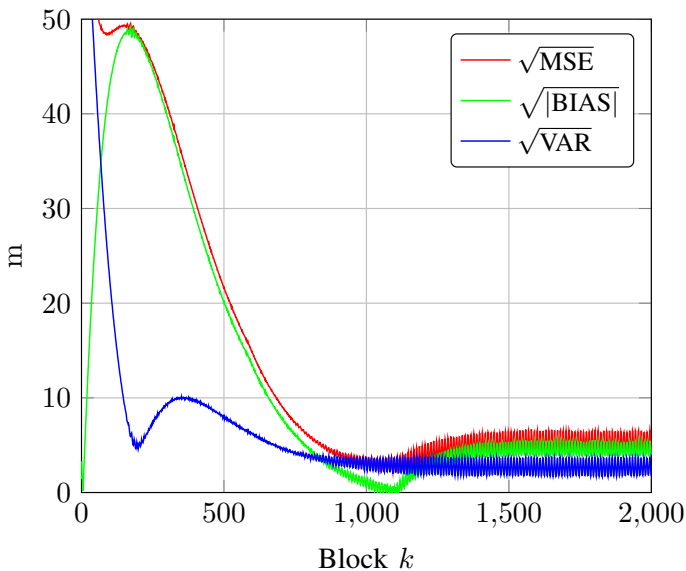


Fig. 6: DLL/PLL Approach

VII. CONCLUSION

In this work, it was shown that unbiased ranging with extremely high precision with one single transmitter is possible in the tracking module of a receiver at moderate complexity. This result was achieved by modeling the carrier phase as an exact function of the propagation delay parameter in the statistical model of the receive signal. The ambiguity issue was resolved by means of a tracking-based alignment filter and a long integration histogram which assigns probabilities to each ambiguity. It was observed that in a satellite-based synchronization and positioning application (GPS) the presented approach significantly outperforms state-of-the-art ranging methods (DLL/PLL) with respect to the RMSE.

REFERENCES

- [1] G. Seco-Granados, J.A. López-Salcedo, D. Jumenez-Baños and G. López-Risueño, "Challenges in Indoor Global Navigation Satellite Systems," *IEEE Signal Processing Magazine*, vol. 29, no. 2, pp. 108–131, 2012.
- [2] P. Misra and P. Enge, "Global Positioning System - Signals, Measurements, and Performance", Second Edition, *Ganga-Jamuna Press*, 2006.
- [3] G. Blewitt, "Carrier Phase Ambiguity Resolution for the Global Positioning System Applied to Geodetic Baselines up to 2000 km," *Journal of Geophysical Research*, vol. 94, no. B8, pp. 10187–10203, 1989.
- [4] P. Teunissen, "Least-Squares Estimation of the Integer GPS Ambiguities", Invited lecture, Section IV "Theory and Methodology," *Proc. of Gen. Meet. of the Int. Assoc. of Geodesy*, Beijing, China, pp. 1-16, 1993.
- [5] P. Teunissen, "A new method for fast carrier phase ambiguity estimation," *Proc. of IEEE Pos., Loc. and Nav. Symp. (PLANS)*, Las Vegas, USA, pp. 562-573, 1994.
- [6] P. Teunissen, "The least-squares ambiguity decorrelation adjustment: a method for fast GPS ambiguity estimation," *Journal of Geodesy*, vol. 70, pp. 65-82, 1995.
- [7] P. Teunissen, "Statistical GNSS carrier phase ambiguity resolution: A review," *Proc. of the 1-th IEEE Workshop of Statistical Signal Processing (SSP)*, pp. 4-12, 2001.
- [8] C. Günther, P. Henkel, "Integer Ambiguity Estimation for Satellite Navigation," *IEEE Transactions on Signal Processing*, vol. 60, no. 7, pp. 3387-3393, 2012.
- [9] S. M. Kay, "Fundamentals of Statistical Signal Processing: Estimation Theory," *Prentice Hall*, 1993.
- [10] B. Ristic, S. Arulampalam and N. Gordon, "Beyond the Kalman Filter - Particle Filters for Tracking Applications," *Artech House Inc.*, 2004.
- [11] A. Doucet and A. Johansen, "A Tutorial on Particle Filtering and Smoothing: Fifteen Years later," *Oxford Handbook of Nonlinear Filtering*, *Oxford University Press*, 2011.
- [12] A. Kong, J. Liu and W. Wong, "Sequential imputations and Bayesian missing data problems," *Journal of the American Statistical Association*, vol. 89, no. 425, pp. 278–288, 1994.
- [13] A. Doucet, S. Godsill and C. Andrieu, "On sequential Monte Carlo sampling methods for Bayesian filtering," *Statistics and Computing*, vol. 10, pp. 197–208, 2000.
- [14] N. J. Gordon, D. J. Salmond and A. F. M. Smith, "Novel approach to nonlinear/non-Gaussian Bayesian state estimation," *IEE Proc. F Radar Signal Process.*, vol. 140, no. 2, pp. 107-113, 1993.
- [15] T. Li, T. P. Sattar, Q. Han and S. Sun, "Roughening Methods to Prevent Sample Impoverishment in the particle PHD filter," 16th International Conference on Information Fusion (FUSION), 2013.
- [16] K. Borre, D. M. Akos, N. Bertelsen, P. Rinder, S. H. Jensen, *A Software-Defined GPS and Galileo Receiver: A Single-Frequency Approach*, Birkhäuser Boston, 2007.